CHALMERS TEKNISKA HÖGSKOLA
Institutionen för Termo- och Fluiddynamik

CHALMERS UNIVERSITY OF TECHNOLOGY
Department of Thermo and Fluid Dynamics

COMPUTER AND EXPERIMENTAL EVALUATION OF DRAG REDUCTION OF BLUNT BODIES AT SUPERSONIC SPEEDS BY COUNTERFLOW COMBUSTION - CONCEPT OF A ”FLAME” SPIKE

Valeri I. Golovitchev

and

Pavel K. Tretjakov

Contract SPC 00-4011

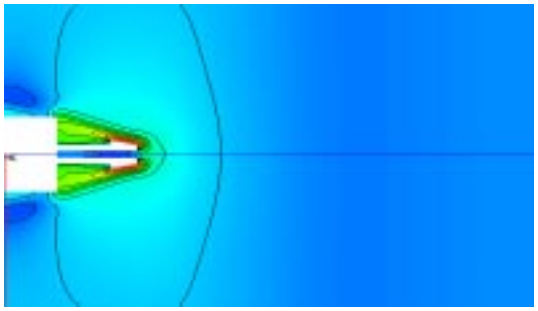

Göteborg
April - May 2001

Report Date *("DD MON YYYY")* 28062001	Report Type Final	Dates Covered (from... to) *("DD MON YYYY")*

Title and Subtitle Computer Evaluation of Drag Reduction Effect for Blunted Bodies at Supersonic Speeds by Counterflow Combustion	**Contract or Grant Number** F61775-00-WE011
	Program Element Number
Authors Valeri, Golovitchev I	**Project Number**
	Task Number
	Work Unit Number
Performing Organization Name(s) and Address(es) Chalmers University of Technology Hoersalsvaegen 7 Goeteborg SE-412 96 Sweden	**Performing Organization Number(s)**
Sponsoring/Monitoring Agency Name(s) and Address(es) EOARD PSC 802 BOX 14 FPO 09499-0200	**Monitoring Agency Acronym**
	Monitoring Agency Report Number(s)

Distribution/Availability Statement
Approved for public release, distribution unlimited

Supplementary Notes

Abstract
This report results from a contract tasking Chalmers University of Technology as follows: The contractor will provide the following a) A theoretical/computational background to evaluate drag reduction effect for different kinds of "flame" spikes in the range of M=2-6 free stream conditions; b) Results to determine energy release conditions leading to the stable flow regimes; c) Experimental information to illustrate drag reduction effect for bodies of particular geometries and specific heat releases; d) Software that can be used to search for new effective fuel compositions; e) Render necessary assistance in performing similar computations or experiments, if requested; and f) Limits of the concept applicability.

Subject Terms
EOARD; Aerodynamics; Combustion; Drag Reduction

Document Classification unclassified	**Classification of SF298** unclassified
Classification of Abstract unclassified	**Limitation of Abstract** unlimited
Number of Pages 23	

REPORT DOCUMENTATION PAGE

Form Approved OMB No. 0704-0188

Public reporting burden for this collection of information is estimated to average 1 hour per response, including the time for reviewing instructions, searching existing data sources, gathering and maintaining the data needed, and completing and reviewing the collection of information. Send comments regarding this burden estimate or any other aspect of this collection of information, including suggestions for reducing this burden to Washington Headquarters Services, Directorate for Information Operations and Reports, 1215 Jefferson Davis Highway, Suite 1204, Arlington, VA 22202-4302, and to the Office of Management and Budget, Paperwork Reduction Project (0704-0188), Washington, DC 20503.

1. AGENCY USE ONLY (Leave blank)	2. REPORT DATE	3. REPORT TYPE AND DATES COVERED
	28-June-2001	Final Report

4. TITLE AND SUBTITLE

Computer Evaluation of Drag Reduction Effect for Blunted Bodies at Supersonic Speeds by Counterflow Combustion

5. FUNDING NUMBERS

F61775-00-WE011

6. AUTHOR(S)

Professor Golovitchev I Valeri

7. PERFORMING ORGANIZATION NAME(S) AND ADDRESS(ES)

Chalmers University of Technology
Hoersalsvaegen 7
Goeteborg SE-412 96
Sweden

8. PERFORMING ORGANIZATION REPORT NUMBER

N/A

9. SPONSORING/MONITORING AGENCY NAME(S) AND ADDRESS(ES)

EOARD
PSC 802 BOX 14
FPO 09499-0200

10. SPONSORING/MONITORING AGENCY REPORT NUMBER

SPC 00-4011

11. SUPPLEMENTARY NOTES

12a. DISTRIBUTION/AVAILABILITY STATEMENT

Approved for public release; distribution is unlimited.

12b. DISTRIBUTION CODE

A

13. ABSTRACT (Maximum 200 words)

This report results from a contract tasking Chalmers University of Technology as follows: The contractor will provide the following a) A theoretical/computational background to evaluate drag reduction effect for different kinds of "flame" spikes in the range of M=2-6 free stream conditions; b) Results to determine energy release conditions leading to the stable flow regimes; c) Experimental information to illustrate drag reduction effect for bodies of particular geometries and specific heat releases; d) Software that can be used to search for new effective fuel compositions; e) Render necessary assistance in performing similar computations or experiments, if requested; and f) Limits of the concept applicability.

14. SUBJECT TERMS

EOARD, Aerodynamics, Combustion, Drag Reduction

15. NUMBER OF PAGES

23

16. PRICE CODE

N/A

17. SECURITY CLASSIFICATION OF REPORT	18. SECURITY CLASSIFICATION OF THIS PAGE	19, SECURITY CLASSIFICATION OF ABSTRACT	20. LIMITATION OF ABSTRACT
UNCLASSIFIED	UNCLASSIFIED	UNCLASSIFIED	UL

Contents

Abstract

This report presents the results of research project with the aim of evaluating the efficiency of energy deposition by combustion upstream blunt bodies in supersonic Mach number 2.0-5.0 air streams. At these conditions, considerable wave drag reduction with a high efficiency of the energy utilization has been demonstrated recently experimentally (see [2] and in the modeling (see [2], [3], [4]). In the most discussions, the energy source is supposed to be attributed to the focused optical (laser) or microwave discharges with an important role of charged particles produced by discharges. For example, it has been claimed in [11] that the presence of only one (!?) electron per 10^7 neutral particles can lead to substantial reduction of both viscous and pressure drag.

The objective of this study is to assess the feasibility of utilizing the thermal energy of counterflow combustion realized using a blunt body with a smaller diameter pipe working as the aerodynamic spike injecting combustible gases upstream the supersonic flow. At these conditions, the charged particles are not formed, and, drag reduction, if confirmed, could be proven not to be the plasma specific phenomenon.

First of all, the experimental evidences of drag reduction by counterflow combustion in supersonic stream are presented. The procedure and hardware used in experiments is described as well. Then, to perform the problem numerical study based on the solution of full Navier-Stokes equations, the KIVA-3 reactive flow computer code has been modified to simulate the counterflow combustion in the M=2.0 supersonic stream using the detailed chemistry approach. In this study, both experimental and theoretical, the hydrogen/air mixture has been analyzed. The results illustrate the considerable effect of the counterflow combustion on a flow structure before the blunt body in the M=2.0 supersonic stream. However, the intensity of heat release appeared not to be sufficient enough to generate a more effective ”air spike” flow structure typical of application of the powerful optical (laser) discharge. To increase the energy release rate, the kinetics of the gasified boron-based hydrocarbon fuel composition has been analyzed. The chemical mechanism has been constructed, and its more high combustion intensity is demonstrated. The important role of a conical tip of the spike for flame stabilization has been also demonstrated.

The direct measurement data of drag reduction by counterflow hydrogen combustion in M=2.0-2.5 air streams are presented and discussed together with the numerical predictions. These results confirm that the ”flame spike” could be an effective means of drag reduction of blunt bodies in supersonic flows.

1.1 Introduction

The concept of structural aerodynamic spike is an effective means to reduce the pressure drag of blunt bodies in supersonic stream. The example of the concept realization is, e.g., the Trident D-5 missile which flying distance was thus increased by 550 km. Other applications are also conceivable.

In the presence of the structural spike, the flow structure is characterized by the presence of the oblique shock and the recirculation zone forming an aerodynamic body profile similar to that of a contoured body. If the spike has a non-optimal length (e.g. too long), the truncated recirculation zone forms (see Fig.1.1), and as far as the oblique shock is stabilized above the front boundary of this zone, drag reduction effect will be moderated.

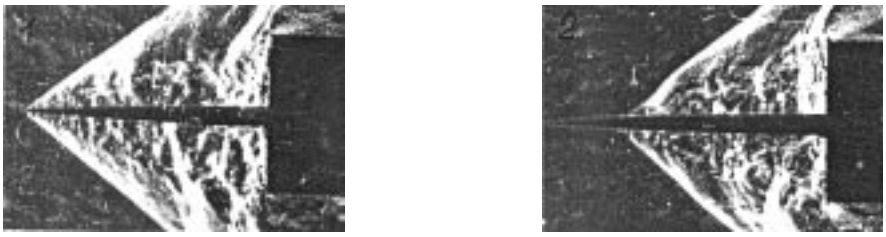

(a) (b)

Figure 1.1: Supersonic flow, M_∞=2.0, structures before a blunt body with a structural spike. Two types (depending on the spike length) of flow separation has been observed: a) the leading-edge and b) delayed separations.

Drag reduction is more related to the problem of construction of a body surface of minimum drag. Among possible analytical solutions, in a class of axysimmetric bodies, there is the solution with a singularity of the body surface that is, in fact, a structural spike. Due to a formal similarity between momentum, mass, and energy conservations, it is possible to show that the drag reduction effect can be achieved by varying momentum, mass, and energy, i.e. mass or energy "spikes" are conceivable. The effect is dependent on the type and size of non-uniformity of the flow around the body. The wake-like non-uniformity, produced, for example, by the structural spike due to non-slip velocity conditions, forms stable flows with the front recirculation zones that reduces drag. On the contrary, the jet-type non-uniformity (produced, if the body has a recess or a blind hole on the front surface) leads to non-steady oscillating flow regimes used in acoustic generators/ resonant tubes.

Some examples of such a generalized spike concept applications are presented below. In Fig.1.2a, the effect of the structural spike is simulated by a bead projected upstream the supersonic M=2.0 flow. The sub-sonic wake behind the bid effectively forms the wake-like non-uniformity of the velocity profile. The effect of such a "spike" becomes well pronounced when the bid reaches the distance similar to the "optimal" length of the spike. The injection of mass can result in the same effect. In Fig.1.2b, the drag reduction is illustrated by Shkval, a cone-shaped rocket-torpedo that travels within a supercavitating bubble flow produced with the help of its own engine exhaust.

The further development of the idea has lead recently to the "air-spike" concept implemented in two different ways by Myrabo [1] and Tretjakov, et al. [2]. The air spike can be formed by concentrated energy (an electric arc plasma torch in the Myrabo's case, a repetitive-pulse laser beam in the case of Tretjakov et al., see Fig.1.2c) projected forward off a moving body producing a "tunnel" of low density, reduced pressure hot air in the shape of a paraboloid of revolution.

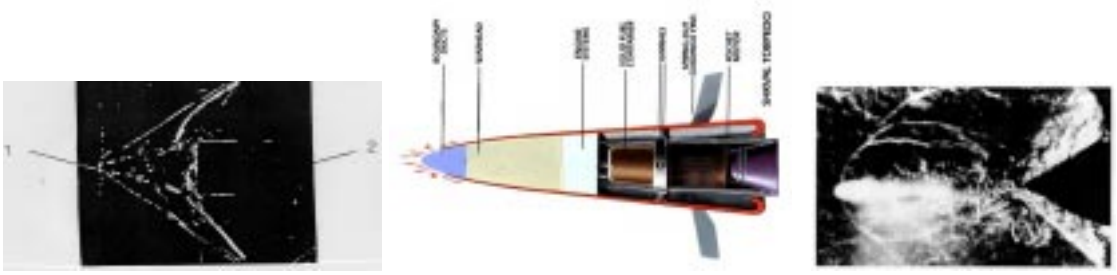

(a) (b) (c)

Figure 1.2: a) Simulation of the structural spike effect by projecting a bid upstream a supersonic M=2.0 flow. b) Drag is reduced by creating a local "envelope" of supercavitating bubbles of gaseous combustion products in which the weapon exceeds a speed 230 mph - a "bubble" spike. c) Schlieren image illustrating Tretjakov et al. air-spike concept realization by concentrating a laser energy before the body in the M=2.0 flow.

Such a "spike" has important advantages over a structural spike due to the fact that air density behind the blast wave is lower than that behind the shock wave. The level of the drag reduction in the supersonic M=2.0 flow can reach $\sim$ 50% of the baseline drag. The effect depends also on the relative "hot spot" position with respect to the body, the "hot" spot size, and M number of the free stream.

Counterflow combustion, as proven in [5] and illustrated in Fig.1.3a-c, tends to weaken (or nearly suppress) the shocks near the blunt body face, thus reducing the drag. In this case, the spike is used to be an injector through which the combustible gas is injected upstream the supersonic flow. The positive effect of such a "flame spike" has been validated both theoretically and experimentally and some measurement data are presented in Fig.1.4 for different (including projectile) geometries.

The combined effect of the structural and "flame" spikes is well illustrated in Fig.1.4a, in which one can see that the drag reduction in the presence of counterflow combustion is better

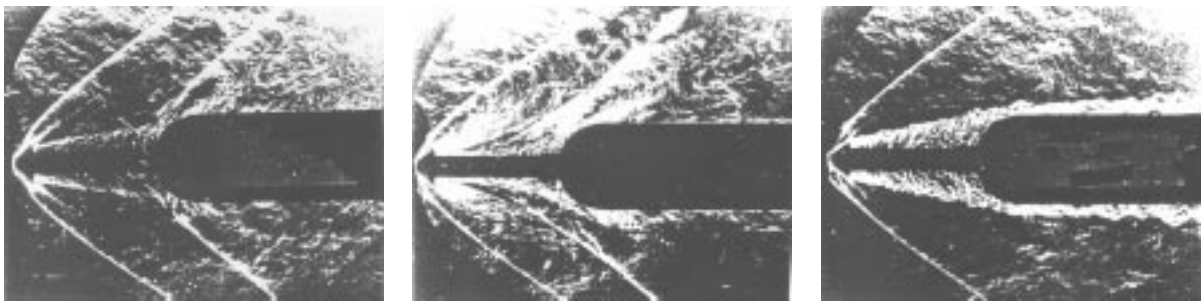

(a) (b) (c)

Figure 1.3: The M=2.0 flow structures: a) in the absence of counterflow injection, b) in the presence of inert gas injection, $\bar{G}_{H_2}$=0.002, and c) in the presence of counterflow combustion, $\bar{G}_{H_2}$=0.002. The hydrogen mass flow rate amounts to 0.2% of the air mass flow rate through the body cross section.

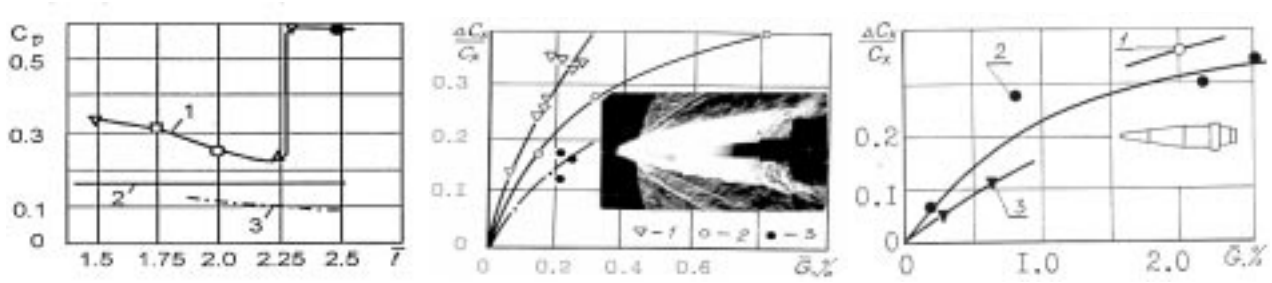

(a) (b) (c)

Figure 1.4: a) The pressure drag vs the structural spike length for the blunt cylinder at M=2.0 flow: 1- pressure drag, 2- base drag, 3- total drag with hydrogen combustion. The pressure drag as a function of a relative mass flow rate, G, for fuels with different heat release in combustion, b) for the model geometry: 1- H_u=120 MJ/kg, 2- H_u=16.7 MJ/kg, 3- H_u=13.4 MJ, c) for real rounds: 1- H_u=16.7 MJ/kg, 2- H_u=13.6 MJ/kg, 3- H_u=9.0 MJ. Low heat values correspond to solid propellants used in the nose gas generator.

pronounced and less susceptible to change in the case, when the structural spike length becomes non-optimal. The Fig.1.4b illustrates that the drag reduction effect can be achieved using very low mass flow rates of combustible gases, and is better pronounced for higher energy density materials. In all illustrations, the relative mass flow rate is the ratio of the injected fuel mass flow rate to the air mass flow rate through the body cross section area. As follows from Fig.1.4a, the concept proposed seems to be more efficient than the well-known drag reduction means using base burning. A wide range of drag variation opens perspective to realize a guided flight using low fuel mass flow rate counterflow combustion.

The flame spike, if applied to a supersonic cruise missile, could reduce drag, thus, preventing deceleration of the vehicle driven by a relatively low power engine with an additional benefit of the spike ”products” can envelope the missile in a film of slightly ionized gas which would be impervious to radar pulses, thereby rendering it electronically ”invisible”. The infra-red penalty at a close range would be significantly offset by the high speed of the flight. The missile could be initially accelerated using a conventional solid propellant booster.

1.2 Description of Work

The purpose of the project was to achieve as follows:

- Obtain via direct measurements the data confirming the ability of counterflow combustion to reduce drag of blunt bodies in supersonic M=2.0-2.5 air streams,
- Present the theoretical background to evaluate the drag reduction effect of counterflow combustion,
- Determination (experimentally or theoretically) of stable energy release conditions in high speed flows,
- Present information available and search for new, more effective than hydrogen, fuel compositions,
- Study of combustion completeness and possible positive effect optimization.

1.3 Experimental Study

The M=2.0 wind tunnel of the Institute for Pure and Applied Mechanics of Siberian Branch of Russian Academy of Sciences, Novosibirsk has been used in the flame spike concept validation. The detailed description of the hardware can be found elsewhere, and a brief description of the particular experiments is given below.

In Fig. 1.5a, it is shown the experiment scheme enabling one to study the flow structure in the presence of the structural spike, the hysteresis phenomena- the transition from one flow separation pattern to another one when the spike length is varied, as well as the effects of the mass supply through the spike and combustion on the flow structure and drag. The spike hysteresis effect was specially investigate ddue to a possible consequence for the moving body with the spike to have different drag depending on whether the body accelerates or decelerates.

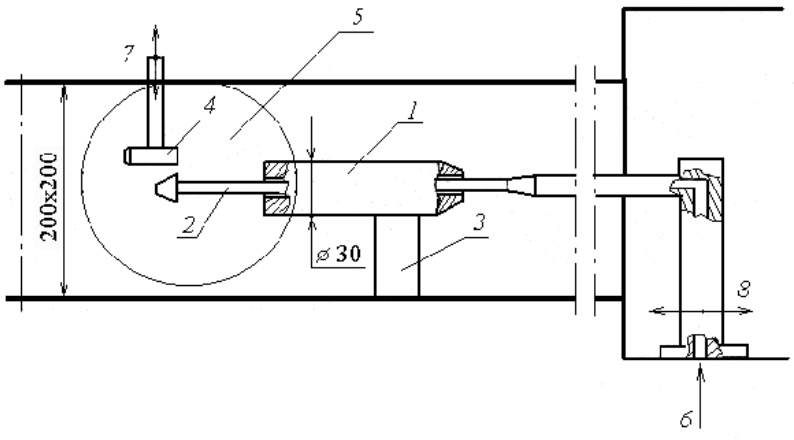

(a)

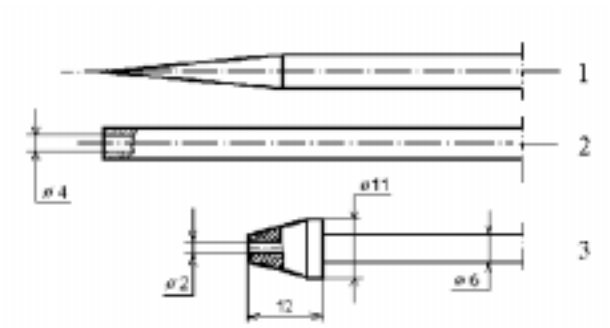

(b)

Figure 1.5: a) Model in a test section of the wind tunnel. Flow conditions: M=2.0-2.5, Re $\approx 10^7$. Notations: 1- model, 2- aerodynamic spike, 3- model aft mounting sting, 4- pilot ignition device, 5- optical window, 6- reacting gas supply, 7- towards the mechanism of a vertical displacement of the pilot ignitor, 8- towards the mechanism of a horizontal displacement of the spike. b) Aerodynamic spikes of different shapes:1- sharp end spike, 2- pipe, 3- pipe with a conic tip.

The aerodynamic spike can be moved along the model axis with the help a coordinate appliance-

the mechanism for a horizontal displacement. The tested aerodynamic spikes of different shape are presented in Fig.1.5b. The spike supplying gases may be argon, hydrogen and air. The experiments with hydrogen injection followed by combustion were carried out as well. Pressure was measured on the face surface of the model with the help of inductive gauges in locations along the radius and recorded by the potentiometer. The spike gas flow rate was measured by the standard gauge based on the diaphragm pressure drop. The displacement speed of the spike accounted for approximately 1 mm/s. The flow regime change was registered with the help of optical observation of the flow structures through the windows using the Töpler's device as well as by pressure measurements along the model face surface.

To initiate counterflow combustion, a microramjet pilot device (see Fig.1.6a) has been used as a source of high temperature products of hydrogen-air combustion. This device operated reliably within the range of M=2.0-2.5. The rich flame quenching regime did not take place within the limits of maximal possible hydrogen mass flow rate through the igniter ($\sim$ 0.2 g/s) determined by the design peculiarities. Fig.1.6b illustrates the ignition device operation. Ignition of the main hydrogen injected from the spike was occured by means of the microramjet device movement towards the hydrogen injection position. After hydrogen ignition, the igniter was removed.

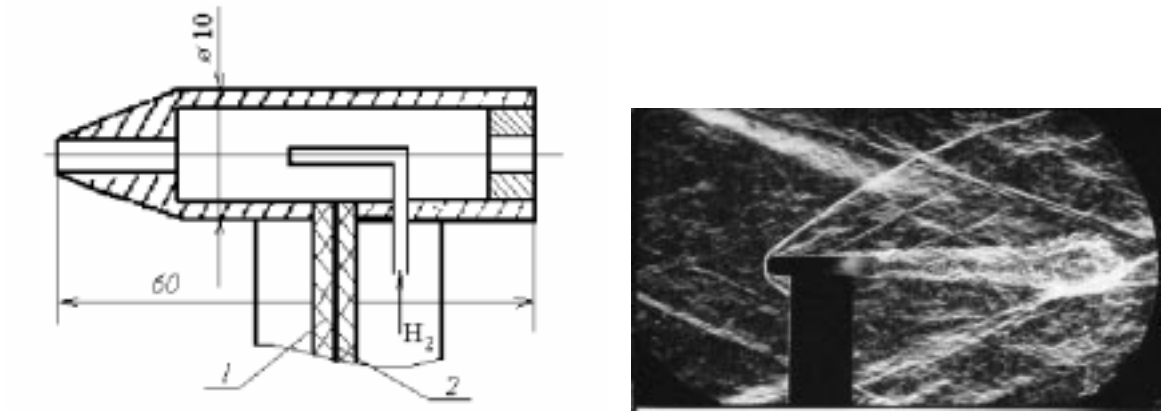

(a) (b)

Figure 1.6: a) Schematic of the pilot ignition device (1- insulator, 2- ignition spark electrodes) and b) visualization of its operation.

A few technical realizations for combustion initiation were considered. They were based on the application of small pyrotechnic ignition cartridge (using silane, SiH_4) and a special realization (see [5]) of the resonance-igniter concept for gas heating in a closed end duct similar to the process in the resonant tubes.

Hydrogen was the fuel of choice because of its high energy release rate and because of hydrogen can be formed in a considerable amount in the pyrolysis of practical hydrocarbon fuels (see, e.g., [7]). First of all, the positive effect of counterflow hydrogen combustion on drag reduction in supersonic M=2.0-2.5 flows has been directly measured and the data are summarized in Fig.1.7. From these data, one can conclude that drag of the blunt body with the structural spike can be reduced to 60 % of the baseline drag when using injection and combustion of a small amount of hydrogen. The relative drag reduction in Fig.1.7 is presented as a function of a parameter which is a product of the relative mass flow rate $\bar{G}$ and the relative heat addition H_o/C_pT_o, where H_o is the combustion heat release. The positive effect of drag reduction by counterflow combustion is comparable with the effect achieved with the help of optical (laser) discharge (see [8]) for the

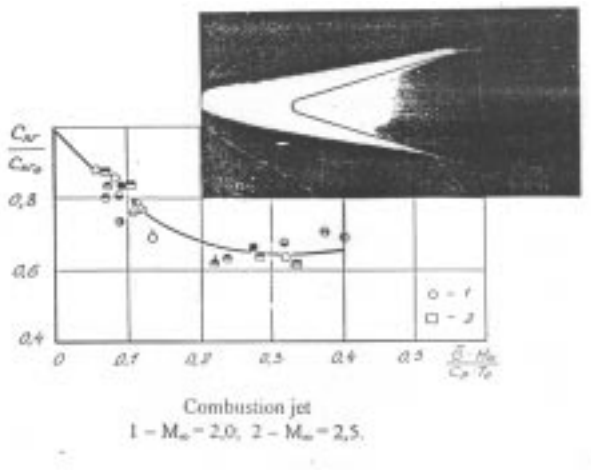

Figure 1.7: Drag reduction effect of counterflow hydrogen combustion in supersonic M=2.0-2.5 streams for blunt bodies of different shapes (cylinder and hemisphere+ cylinder) with the structurlal spikes used as the fuel injector.

same flow conditions.

Then, a series of experiments was carried out that enabled one to determine the minimum sizes of the blunt body with the aerodynamic spike that makes it possible to realize the steady-state hydrogen combustion in air stream with parameters M_∞=2.0-2.5, P_{tot}=2.5-4.5 atm, T_{tot}=300 K. The results are summarized in Fig.1.8. Fig.1.8a illustrates the relationship between

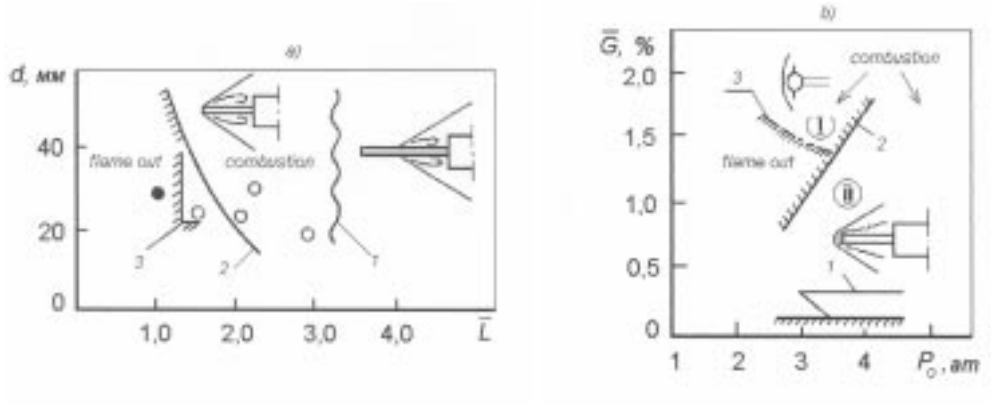

(a) (b)

Figure 1.8: Regions (in the $d - \bar{L}$ and P_o-$\bar{G}$ planes) of hydrogen steady counterflow combustion in the supersonic, M_∞=2.0 stream: a) the minimum diameter of the body, and the spike length; b) the hydrogen mass-flow rate and the total pressure. Boundaries of the flame blow-off: 1 - a "lean" flame blow-off, ($\lambda > 1.0$), 2- a "rich" flame blow-off, ($\lambda < 1.0$), 3 - a "lean" flame blow-off for a free counterflow jet.

the body diameter, d, and the dimensionless length of the structural spike, $\bar{l} = L/d$, where L is the spike length, in the region of stable combustion. The boundary 3 corresponds to the flame which is stabilized by a separation zone formed by a free hydrogen jet not connected with the

separation zone in front of the blunt body with the spike. The "lean" flame blow-off takes place when the spike is longer than the optimal one. Fig. 1.8b shows the regions of stable combustion in the $\bar{G} - p$ plane: I is the boundary of the stable counterflow combustion for a free jet, II is the stabilization region for the blunt body with the spike. This region has two boundaries marked by 1 and 2. The flow structures corresponding to counterflow hydrogen injection and combustion are presented in Figs 1.9-1.10.

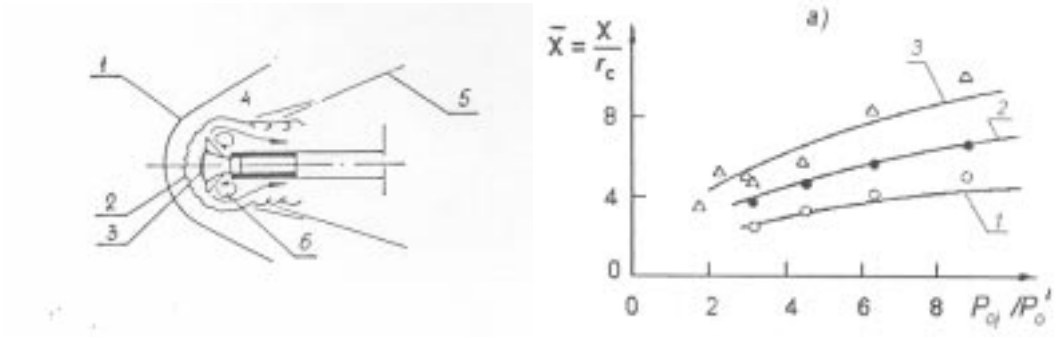

(a) (b)

Figure 1.9: a) Gasdynamic M=2.0 flow structure for the inert cointerflow jet: 1- bow shock, 2- contact surface, 3- shock of the jet, 4- region of flow expansion, 5- re-attachment shock, 6- flow separation zone, 8- injector. b) Dependence of the main geometrical parameters of the inert jet on the gas injection pressure.

Data presented in Fig.1.9 correspond to the case of the inert jet, in Fig.1.10 - to the case of counterflow combustion. These data were obtained with the help of schlieren photographs of the fluid structure. Geometrical characteristics of both, inert and reacting counterflow jets are well generalized using the dimensionless parameter: a ratio of the total pressure in the jet, P_{oj} to the pressure behind the normal shock at the parameters of the free stream, P_o'. The effect of

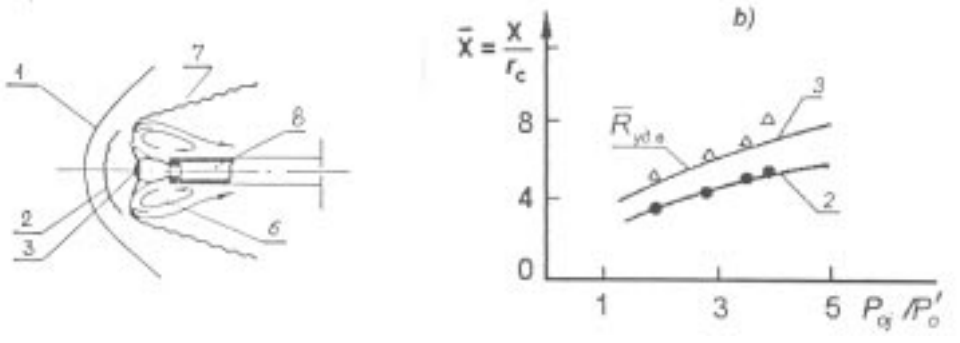

(a) (b)

Figure 1.10: a) Gasdynamic M=2.0 flow structure for the reacting cointerflow jet: 1- bow shock, 2- contact surface, 3- shock of the jet, 6- flow separation zone, 7- flame, 8- injector. b) Dependence of the main geometrical parameters of the inert jet on the gas injection pressure.

combustion is well pronounced: for this case, the distance to the normal shock 3 and the contact surface radius 2 are longer than for the inert case due to the lower density in the recirculation zone of the reactive flow. This also means that the shock wave inclination for the case of the reactive flow becomes less that testifies to drag reduction caused by counterflow combustion.

Thus, one can conclude that the possibility of drag reduction using the counterflow combustion in supersonic streams realized in a form of the "flame" spike is confirmed experimentally. The size of the body and and the spike length can be selected to guarantee stable combustion for given free stream conditions. The effects of the mass flow rate and the energy deposition variations for the model fuel (hydrogen) are studied. It has been demonstrated that drag of the blunt body with the "flame" spike in M=2.0-2.5 streams can be reduced up to 60 % of drag of the baseline blunt body with the structural spike. At that, the blunt body shape does not play an

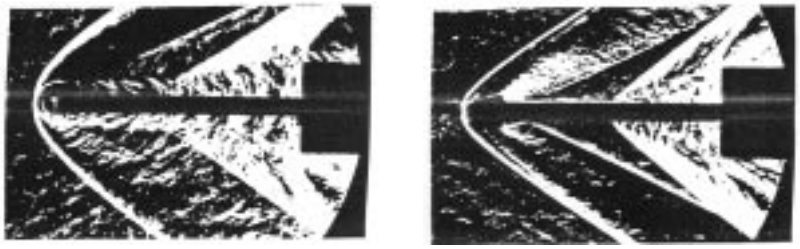

(a) (b)

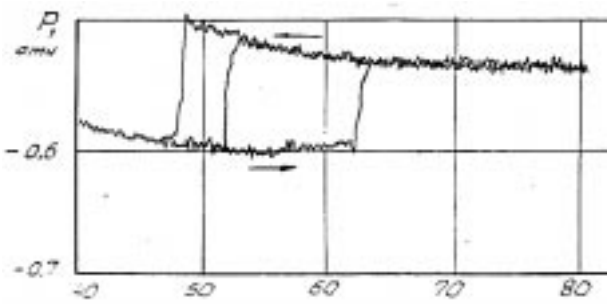

(c)

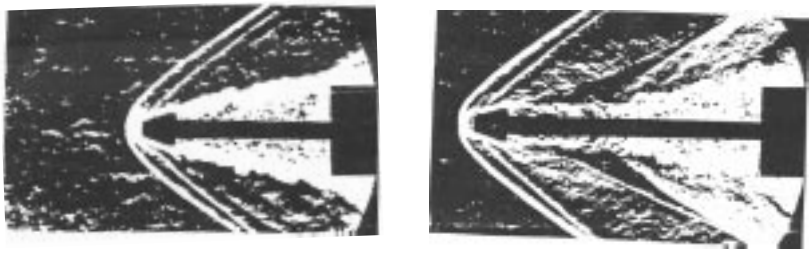

(d) (e)

Figure 1.11: Spike hysteresis- M=2.0 flow structures and pressure diagram. Flow structures for a) the optimal length structural spike, b) the long structural spike, d) the short length flame spike ($\bar{G}$=0.015), e) the long flame spike. In c) it is presented the total pressure vs spike length (in mm) record.

essential role. The interesting feature of the experimental data obtained is the effect moderation (see Fig.1.7), if the fuel amount injected or the amount of energy released will exceed some specific values. This effect will be discussed later on.

The spike hysteresis effect is very important for practical application due to the consequence that the moving body with the spike may have different drag depending on whether the body accelerates or decelerates. Information presented in Fig. 1.11 can be used to clarify the matter. Hysteresis was shown to exist between the two types of flow separation caused by the presence of the spike: the first one occurs (see Fig. 1.11a) when the spike has the optimal length, the second one ((see Fig. 1.11b) is typical of the long spike. Due to the hysteresis (see Fig. 1.11c), it is possible to enter the high drag state from low drag at the same spike length, although the reverse is not true. Date presented in Fig. 1.11d-e are characteristic of the counterflow combustion reducing this effect substantially: for two flame spikes of different lengths this is no transition from one flow separation regime to another observe. This explains the results presented in Fig. 1.4 and illustrates the unique feature of the flame spike..

1.4 Theoretical Study

At first, the counterflow combustion in a supersonic flow was studied numerically with the help of a computer code described in [2]. In this case, the effect of combustion has been simulated by introduction of the heat source term in the energy equation. The typical results obtained by applying the code to M=2.5 air flow around a sphere are presented in Fig.1.12. If the heat release of a sufficient intensity was localized in a small region before the blunt body, the flow structure was considerably changed representing a pattern typical of the flow structure in the presence of the structural spike. In this case, one can see a departure of a normal shock from the sphere and its transformation into the oblique shock, thus, reducing drag. The prolate subsonic recirculation zone was predicted (see Fig.1.12b) before the body. This phenomenon attributed to the optical discharge has been described in [4].

Then, the analytical study using the approach proposed by Guvernuk [13] was carried out allowing to conclude that the drag reduction effect is achieved mainly due to the formation of the wake type non-uniformity in the incoming air stream. The initial non-uniformity can be formed by the fuel counterflow injection. In the presence of combustion, this type of non-uniformity can be reinforced or reduced depending on the combustion wave propagation direction and the combustion regime, i.e., deflagration or detonation. It is known that in the detonation regime,

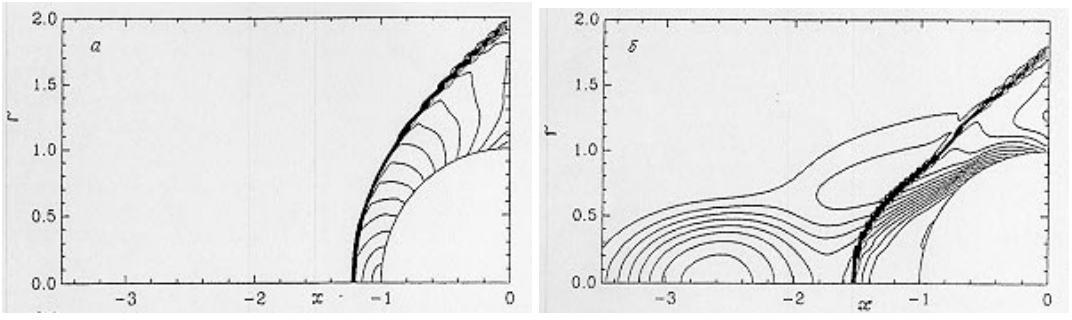

(a) (b)

Figure 1.12: Calculated Mach number (15 isolines ranged between 0.0- 2.5) distributions around a sphere a) without and b) with the energy release zone placed before the body.

combustion products move in the direction of the propagating combustion wave. In the deflagration regime, another situation takes place: gases escaping the combustion zone are moving directly opposite. Using the counterflow gas injection of combustible gases, it is difficult to expect that the detonation regime could be realized. If, in the deflagration regime, counterflow combustion is realized by forming the flame propagating to the body surface, the "flame" spike effect will reinforce the effect of hydrogen injection.

The term "deflagration" summarizes flame propagation regimes corresponding to a low branch of the Hugoniot curve. Recently [7], the enhanced turbulent deflagration mode was numerically predicted in the case of a stoichiometric hydrogen/air mixture under atmospheric conditions when ignition was initiated by a powerful electrical discharge in a duct constructed as a "two-room compartment", where two volumes, donor and receiver, were connected by a narrow passage. The mathematical model and modifications of the KIVA-3 computer code [6] used for numerical simulation are described in [7]. In order to account the effect of turbulence/chemistry interactions, the PaSR (Partially Stirred Reactor) model in a generalized form has been incorporated into a framework of the RNG $k-\epsilon$ turbulence model for reacting compressible gases, to simulation hydrogen counterflow combustion. The brief model description is given below.

1.4.1 Model of turbulent combustion

Most methods in reacting flow modeling involve numerical solutions of the Reynolds-averaged Navier- Stokes (RANS) equations. More sophisticated, but more promising approaches make use of the probability density function (PDF) technique coupled with the large eddy simulation (LES) models. Once the PDF is known, the mean chemical reaction rates can be treated in a closed form, irrespective of complexity of a chemical mechanism. Some methods use a prescribed form of the PDF parameterized by its lower statistic moments, in others, the function is defined by solving the evolutional single-point PDF equation. Both approaches become problematic when applied to complex chemistry. With the assumed PDF method, the choice of the PDF form is quite arbitrary, and, as the number of species grows, this technique leads to an unlimited number of low-moment equations which must be closed and solved. For the direct PDF approach, the problem arises when the unclosed micro- mixing terms are modeled.

Application of another useful idea to turbulence combustion modeling assumes that under high-intensity conditions, turbulence exerts the main impact on the mechanism of turbulence combustion, but the influence of finite-rate chemistry is never negligible. The formation of an archipelago of unburnt gas pockets due to the distorted flame front reconnections can be regarded as a main consequence of the model. In this case, the PaSR (Partially Stirred Reactor) model has been generalized to account for the effect of mixture imperfections on chemical reaction rates.

The model distinguishes (see Fig.1.13a) between the concentration (in mean molar density) an the reactor exit, c^1, the concentrations in the reaction zone, c, and in the feed, c^0. To illustrate the relation between rates of the processes I-II in the reactor, let us analyze the PaSR differential- algebraic problem

$$\frac{c^1-c^o}{\tau}=-\frac{c}{\tau_c},\quad \frac{c-c^1}{\tau_{mix}}=-\frac{c}{\tau_c}, \tag{1.1}$$

where τ is the time step, τ_c is the chemical reaction time, and τ_{mix} is the micro-mixing time.

The equations above (represented graphically in Fig.1.13b), express the idea that combustion in the reactor is a sequential process where mixing is followed by chemical reactions, and that in any moment, the rates of the individual steps are equal. After algebraic manipulations, one can yield the analytical solutions of the linear problem (1.1):

$$\frac{c}{c^1} \;=\; \frac{\tau_c}{\tau_{mix}+\tau_c} \tag{1.2}$$

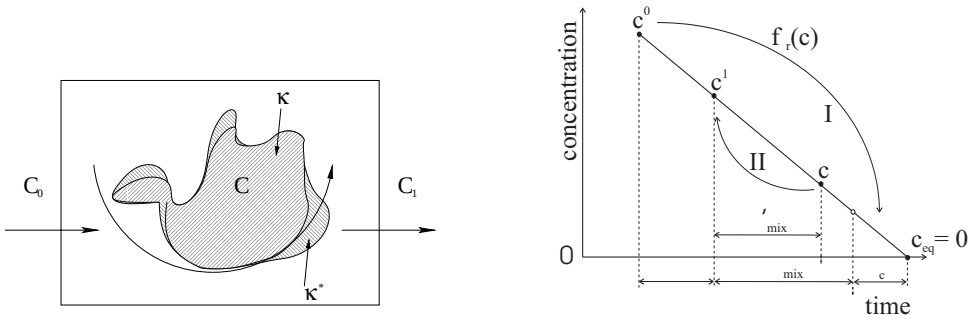

(a) (b)

Figure 1.13: a) The concept of a partially stirred reactor, PaSR. The reaction zone is lined; b) Process rates diagram for the PaSR.

The solution (1.2) shows that the turbulent combustion time is a sum of the mixing and reaction times, if the process is expressed in terms of the reactor output parameters. Thus, the model is similar to turbulent dissipation (or eddy break-up) approach, however, accounting for finite-rate chemistry. Finally, the solution (1.2) can be represented as

$$\frac{c^1 - c^o}{\tau} = -(\frac{c^1}{\tau_c}) \cdot \kappa = -\frac{1}{2} Hm(\frac{c^1}{\tau_c}, \frac{c^1}{\tau_{mix}}), \tag{1.3}$$

where $\kappa = \tau_c/(\tau_{mix} + \tau_c)$, and Hm is a harmonic mean.

The model generalization is equivalent to a substitution of the equations (1.1) for a set of the general PaSR rate balances

$$\begin{aligned} I.\ \frac{c^1 - c^o}{\tau} &= f_r(c), \\ II.\ \frac{c - c^1}{\tau} &= \frac{c^1 - c}{\tau_{mix}} + f_r(c), \end{aligned} \tag{1.4}$$

where

$$f_r(c) = (\nu_r'' - \nu_r')\dot{\omega}_r(c) = term_r^{\oplus} - term_r^{\ominus} \tag{1.5}$$

is the Arrhenius chemical source term separated into production, $term_r^{\oplus}$, and destruction, $term_r^{\ominus}$, rates, ν_r'' and ν_r' are the stoichiometric coefficients of the backward and forward stages, respectively. Species indices are omitted for simplification.

The r-reaction progress variable $\dot{\omega}_r(c)$ is calculated from the mass-action law

$$\dot{\omega}_r(c) = k_r^f(T) \prod_{i=1}^{N_s} (c_i)^{\nu'_{ri}} - k_r^b(T) \prod_{i=1}^{N_s} (c_i)^{\nu''_{ri}},$$

where T is the temperature, k_r^f and k_r^b are the rate coefficients for the forward and backward stages of the reaction, and N_s is the total number of species in the mixture.

The first equation of the system (1.4) represents the chemical step of the operator splitting procedure applied to the species mass balance. The second one is the time dependent species mass conservation equation analogous to that in the PSR model, when the residence time is replaced by the micro-mixing time. From matching the systems (1.1) and (1.4) follows that they

are analogous, if the second equation in the system (1.4) is taken in a steady-state form. Finally, one can get the general rate expression

$$\begin{aligned} \frac{c_s^1 - c_s^o}{\tau} &= f_r(c_s^1) \cdot \kappa = \frac{c_s^o f_r^o}{c_s^o + term_r^{\ominus}\tau + term_r^{\ominus}\tau'_{mix}} \\ &= \frac{1}{2} Hm(\frac{c_s^o f_r^o}{c_s^o + term_r^{\ominus}\tau}, \frac{c_s^o f_r^o}{term_r^{\ominus}\tau'_{mix}}) \end{aligned} \tag{1.6}$$

containing no reaction zone parameters c, which cannot be resolved on a computational grid, but replacing their effect with the rate multiplier $\kappa = \tau_c/(\tau_c + \tau'_{mix})$; $\tau'_{mix} = 1/2Hm(t, \tau_{mix})$. The superscript ^{o} denotes the values at the start of the time integration, while the subscript ^{s} refers to the "reference" species which are equivalent to the "limiting" species of the Magnussen-Hjertager EDC-model.

The formal introduction to the concept of "reference" species facilitating calculations of reaction rates in the multi-stage chemical mechanism can be found in [14]. If $\tau_{mix} \to 0$, the model reduces to the quasi-laminar approach with $c^1 \equiv c$ in the reaction rate terms. Similarly to Eq. (1.3), the arguments of the harmonic mean function in Eq. (1.6) are the reaction rate and the eddy dissipation rate, respectively. In the limit of fast chemistry, i.e., $term_r^{\oplus} \cdot c_s^o = term_r^{\ominus} \cdot c_s^1$, the dissipation rate in Eq.(1.6) reproduces the classic eddy break-up rate, $\sim (c_s^1 - c_s^o)/\tau'_{mix}$.

1.4.2 Definition of micro-mixing time

If the RNG $k-\epsilon$ model is employed, the turbulent viscosity related to k, the turbulent kinetic energy, and ϵ, the dissipation rate of k, is given by the general expression.

$$\mu_t = \mu_l(1 + \sqrt{\frac{c_\mu \rho k^2/\epsilon}{\mu_l}})^2 = \rho(\nu_l + {\nu^s}_t + 2\sqrt{\nu_l {\nu^s}_t}), \tag{1.7}$$

where ${\nu^s}_t$ is the "standard" k-ϵ value of the kinematic viscosity.

The above expression represents contributions of three mechanisms of diffusion transport, molecular, average turbulent, and the additional one responsible for micro-mixing. The model is assumed to be valid across a full range of flow conditions from low to high Reynolds numbers, if k and ϵ are determined from the generalized transport equations,

$$\begin{aligned} \frac{D\rho k}{Dt} &= P - \rho\epsilon + \nabla \cdot [(\frac{\mu_t}{Pr_k})\nabla k] \\ \frac{D\rho\epsilon}{Dt} &= c_{\epsilon 13}(\rho\epsilon)\nabla \cdot \mathbf{U} + \frac{\epsilon}{k}(c_{\epsilon_1} P - c_{\epsilon_2}\rho\epsilon) + \nabla \cdot [(\frac{\mu_t}{Pr_\epsilon})\nabla\epsilon], \end{aligned} \tag{1.8}$$

where P is the production term, given by

$$P = \mu_t[S - \frac{2}{3}(\nabla \cdot \mathbf{U})^2] - \frac{2}{3}\rho k \nabla \cdot \mathbf{U},$$

and S is the mean strain rate, defined as

$$S = \frac{1}{2}(\frac{\partial U_j}{\partial x_i} + \frac{\partial U_i}{\partial x_j})^2$$

Provided that the first two terms in (1.7) contributed to the conventional diffusion transport, the geometrical mean term in the expression can be used to define the characteristic time scale for micro-mixing in the turbulence/chemistry interaction model, if written in a form,

$$\tau_{mix} = 2\sqrt{\nu_l {\nu_t}^s}/k = 2{c_\mu}^{1/2}\tau_k \sim \tau_k, \tag{1.9}$$

where c_μ=0.09, τ_k= $(\nu_l/\epsilon)^{1/2}$ is the Kolmogorov time.

Thus, the sequence of diffusion processes is represented by different, gradient and non-gradient, approaches. Eq. (1.9) can be rewritten using the eddy break-up time definition

$$\tau_{mix} \sim \tau_k = (c_\mu/Re_t)^{1/2} k/\epsilon \tag{1.10}$$

This leads to a correct dependence of τ_{mix} on the Re_t=$\nu_t{}^s/\nu_l$, but its actual value has to be optimized. For a typical Re_t $\sim 10^3$ case, the value is about $0.01k/\epsilon$ used in the modeling. If smallest eddies are enlarged to be resolved by a computer grid, i.e.,

$$\begin{aligned} l_{sgs} &= \int_{1/\Delta}^{\infty} dk k^{-1} E(k) / \int_{1/\Delta}^{\infty} dk E(k) \sim \Delta \\ \nu_{sgs} &= \int_{1/\Delta}^{\infty} dk k^{-1} [k^{-1} E(k)]^{1/2} \sim \epsilon^{1/3} \Delta^{4/3}, \end{aligned}$$

another definition of the micro-mixing time has been used.

$$\tau_{mix} \sim \Delta^{2/3} \epsilon^{-1/3} \tag{1.11}$$

where Δ is the minimal scale resolved on the grid, $E(k) = C\epsilon^{2/3} k^{-5/3}$ is the Kolmogorov energy spectrum. The formula (1.11) renders the model a quality of the SGS (sub-grid scale) approach.

1.4.3 Results and discussion

To account for the hydrogen/oxygen distribution and combustion after hydrogen counterflow injection, both mixing and ignition/combustion processes must be simulated. To simulate the effect of combustion, the reaction mechanism of hydrogen oxidation in air has been constructed. Most of the reactions have been studied experimentally, and the mechanism has previously been used for hydrogen propulsion modeling [9]. The reaction-rate parameters in the form of $k_j = a_j T^{\zeta_j} exp(-E_{aj}/R_o T)$ are taken from different sources and the electronic copy of the mechanism can be found on our web site [10].

Using the reaction mechanism developed, the calculated ignition delay times for stoichiometric hydrogen air mixtures at different initial pressures and temperatures were calculated and compared with the shock-tube experiments. Good agreement has been achieved as illustrated in Fig. 1.14. The main goal in using the detailed mechanism of hydrogen combustion is to

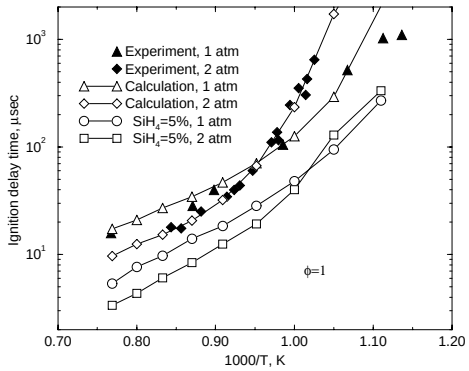

Figure 1.14: Validation of H_2/air ignition chemistry. Ignition promotion and moderation of its dependence on pressure for the stoichiometric mixture by adding a small amount of silane.

correctly reproduce rather ill-ignition conditions above the so-called extended second explosion limit for hydrogen/air mixtures. This effect is well pronounced in the data presented in Fig. 1.14. Due to this effect, the ignition delay for higher pressure which is shorter than the ignition delay for lower pressure at temperatures higher than the explosion limit temperature, becomes longer, if the initial temperatures are lower than the limit. This is why, one can see the intersection of two experimental (for different pressures) curves presented in Fig. 1.14. This phenomenon is likely responsible for deterioration of drag reduction efficiency observed in the experiments (see Fig. 1.7), if larger amounts of hydrogen were injected. As a result, this can lead to the increased pressure level in the ignition zone, thus, worsening auto-ignition conditions. To moderate the ignition delay dependence on pressure, it has been assumed in [12] to make use of silane as the ignition promoter. The measure facilitates the ignition process which, in this case, becomes nearly hypergolic.

The results of 2-D counterflow combustion simulations using the KIVA3 computer code modified to account for detailed chemistry hydrogen/air combustion are presented in Fig. 1.15. In

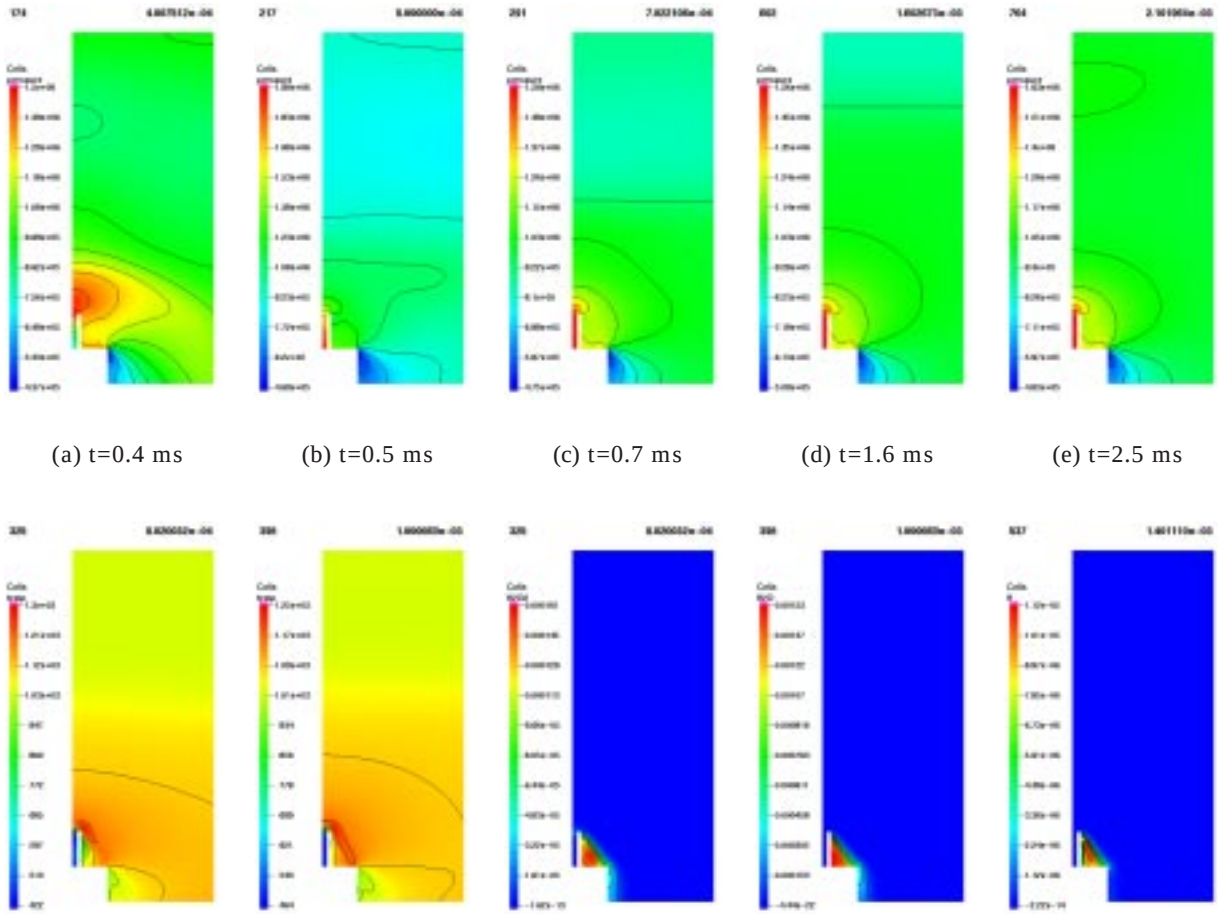

(a) t=0.4 ms (b) t=0.5 ms (c) t=0.7 ms (d) t=1.6 ms (e) t=2.5 ms

(f) t=0.8 ms (g) t=1.0 ms (h) t=1.0 ms (i) t=1.0 ms (j) t=1.0 ms

Figure 1.15: Time development of couterflow H_2/air combustion for the pipe-spike. Plots a)-e) correspond to pressure distributions at different moments; plots f)-g)- to temperature distributions; plots h), i) and j)- to distributions of hydrogen peroxide, water vapor and atomic hydrogen, respectively.

the axisymmetric simulations, a part of a cylinder body of a size 2x2 cm with a structural spike of a length 2 cm was placed in a computation region of a size 8x20 cm. The structural spike was a pipe of the inner radius 0.25 cm, and the outer radius 0.5 cm. Hydrogen has been injected through the pipe with a speed of 50 m/s. The free air stream velocity corresponded to M=2.0 and P_o=1.o atm. Hydrogen ignition has been initiated by two hot spots: the first one was placed inside the pipe (for a short time), and the second one - 0.5 cm below the spike end in the recirculation zone. Transient calculations continued till the steady-state was achieved (but not longer than 10 ms). All this time, hydrogen injection continued, but the external hot spot was supported by the energy source in the course of 1 ms. Within the ignition window, the specific internal energy in the specified mesh cells was increased on each timestep. If the temperature in the ignition cell was in excess of 2000 K before the end of the ignition window, then, in this point, the energy deposition was terminated.

The block-structured mesh KIVA-3 code used, in the modeling, might be considered of only a moderate accuracy for aerodynamic calculations, but such an accuracy seems to be sufficient to simulate the effects of counterflow combustion on the supersonic flow structure. From the results presented in Fig. 1.15, one can conclude that the typical shock structure (see Fig. 1.15a) formed in front of the blunt body at the initial moment was smoothed later on while combustion process was developing (see plots Fig. 1.15b-c). This prediction is in agreement with the experimental observation. From the temperature distributions (see plots in Fig. 1.15f-g), one can see that the flame was stabilized in the frontal recirculation zone formed in the presence of the structural

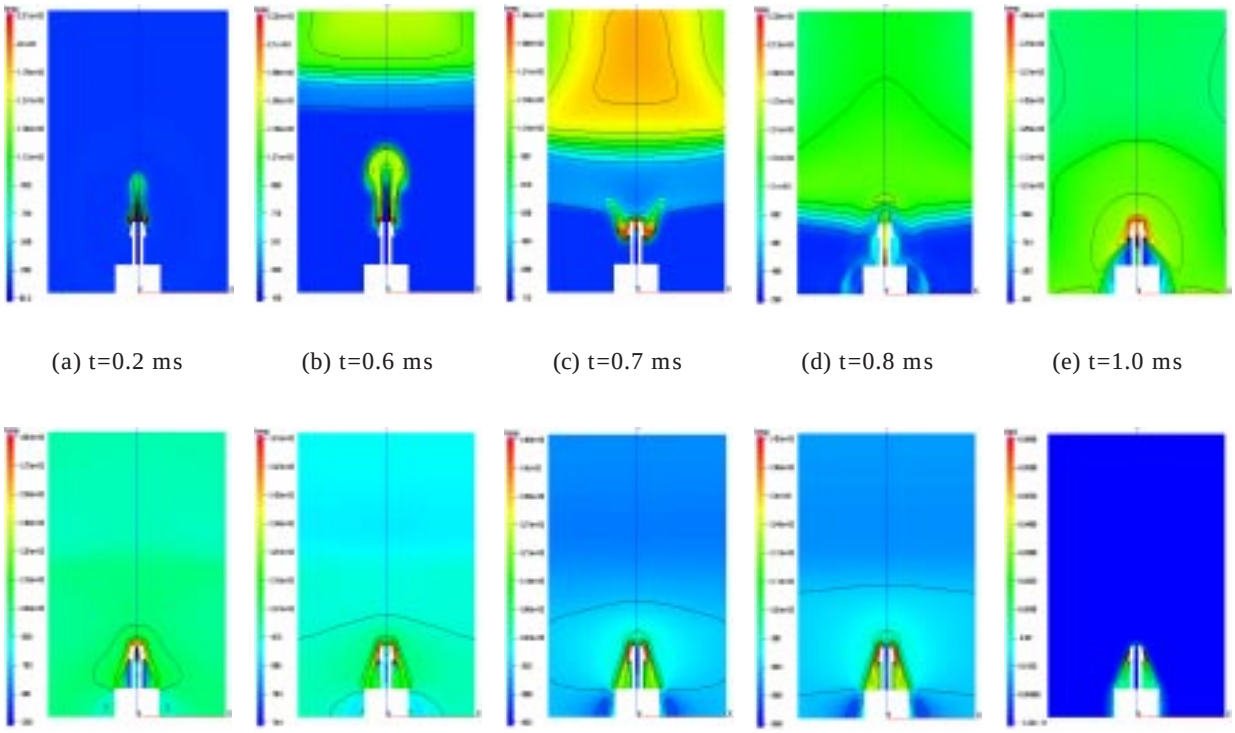

(a) t=0.2 ms (b) t=0.6 ms (c) t=0.7 ms (d) t=0.8 ms (e) t=1.0 ms

(f) t=1.2 ms (g) t=1.4 ms (h) t=1.7 ms (i) t=2.0 ms (j) t=2.5 ms

Figure 1.16: Time development of couterflow H_2/air combustion for the conical tip spike. Plots a)-i) correspond to temperature distributions at different moments; the plot j)- to the distribution of water vapor.

spike. The distributions of intermediate (hydrogen peroxide) species and main (water vapor) combustion products as well as a high concentration of H- radicals show that the heat release takes place only in this region, effectively forming the flame spike structure of the counterflow combustion. The temperature in the reaction zone was predicted to be only $\sim$ 1300 K. The predicted flame shape and position testifies to the fact that combustion takes place in the lean mixture, and the deflagration regime is realized with the flame front moving towards to the body surface. In this case, the reaction products are moving in the same direction as the injected gases, thus, increasing the positive effect of injection. As the high level of temperature in the reaction zone was not achieved at modeling conditions, special measures should be taken to enhance and stabilize combustion. To stabilize the flame in the experiments, a conical tip on the spike end was used. Thus, the spike geometry was modified in the modeling to account for the presence of the tip, and the computation results are presented in Fig. 1.16.

In this modeling, the spike length was increased by 1.5 cm, from which 0.5 cm was a shear of the conical tip. The pipe inner diameter was reduced to 0.2 cm, that allowed to specify a higher injection velocity (200 m/s) without substantial increasing of the hydrogen mass flow rate. The simulation scenario was also changed: hydrogen injection and ignition (see Fig.1.16a) took place in the quiescent atmosphere. Then, at the moment t=0.5 ms the air was set in motion corresponding to M=2.0 and the total pressure P_o= 1.0 atm. The air stream parameters were calculated using the isentropic flow relations for a perfect gas. The air stream formed the region of elevated pressure and temperature which interacted with the developed hydrogen flame as can be seen in Fig.1.16b-c. As the result of the interaction, the flame front was transform into a typical form of a ”butterfly”, the shape of which was observed in the experiments. Then, incoming air flow blew the flame almost away, and combustion continued only in the pipe. Later on (see Fig. 1.16d-e), the hydrogen combustion in the supersonic stream was re-established, and the reaction zone structure rebuilt the configuration typical of the developed flame spike (see Fig. 1.16f-i). Water vapor distribution in Fig. 1.16j illustrates an important role of the tip in the flame stabilization. The higher temperature, 1420 K, was predicted in the reaction zone.

The simulation results, when the hydrogen injection velocity was increased iup to 250 m/s are presented in Fig. 1.17. As a result, the combustion zone became more extended (see Fig. 1.17a), but a character of the flame front interaction with the air stream remain unchanged, e.g., at first, the flame ”butterfly” structure was formed, then, the flame was almost extinguished, and regenerated once again (see Fig. 1.17b-e). The temperature maximum in the reaction zone

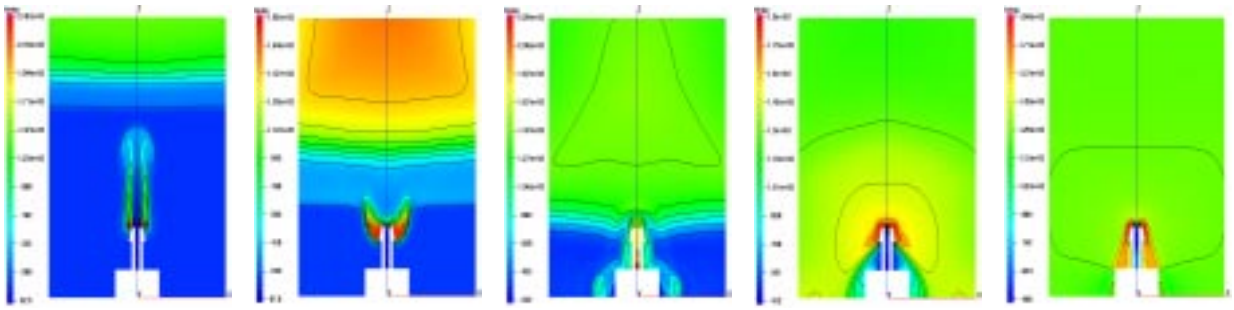

(a) t=0.6 ms (b) t=0.7 ms (c) t=0.8 ms (d) t=1.0 ms (e) t=2.5 ms

Figure 1.17: Time development of couterflow H_2/air combustion for the conical tip spike. Hydrogen njection velocity is equal to 250 m/s. Plots a)-i) correspond to temperature distributions at different moments.

reached 1840 K, and combustion was well stabilized in the recirculation zone behind the tip. One can expect than this tendency could be extrapolated to the higher hydrogen injection velocities. However, it requires further reduction of the pipe inner size that arises a problem of the mesh resolution in simulations of a moderate accuracy.

As a conceivable measure of temperature increase in the combustion zone could be considered an addition of boron to hydrogen injected through the spike. The boron effect on the hydrogen combustion has been studied using the time-dependent reaction code Senkin of the Chemkin library, and the results of computations are presented in Fig. 1.18. The extended chemical me-

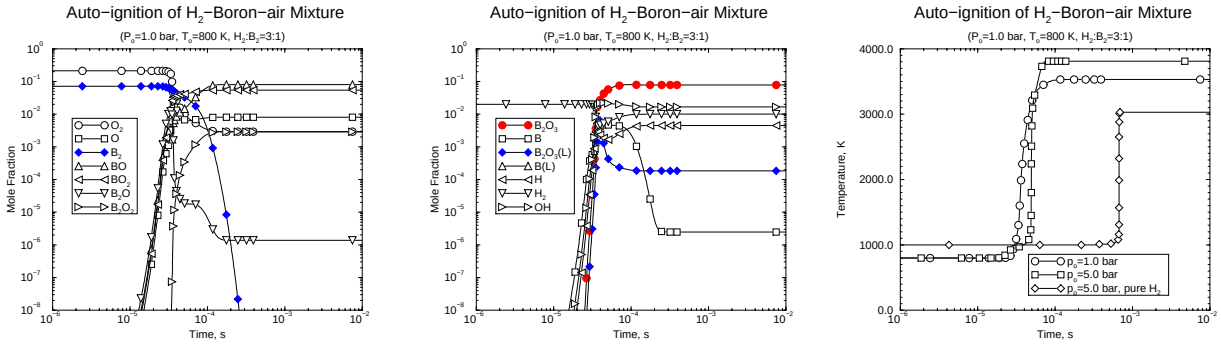

(a) (b) (c)

Figure 1.18: a) Selected concentrations of combustion products vs time histories, b) selected concentrations of combustion products vs time histories, c) illustration of reduced ignition delay and increased heat release when compared with parameters of similar stoichiometric hydrogen/air mixture.

chanism accounting for the presence of boron vapor in the mixture can be found on our web site [10]. The comprehensive mechanism of hydrogen/boron combustion consists of 64 elementary reactions between 22 species including B, B_2, BO, BO_2, B_2O, B_2O_2, B_2O_3, B_2O_3(L), B(L), L denotes the liquid phase. The auto- ignition of H_2/boron mixture (3:1, in mole numbers) was studied within the initial temperature range of 700- 900 K, and the pressure range of 1- 5 bar. In the Fig. 1.18a-b, one can see that the concentration of B_2O_3 in the gas phase exceeds that of B_2O_3(L) at the equilibrium state. However, there is a moment in the development of the auto-ignition process development, when these phases are predicted in comparable quantities. Such a presence of the liquid phase in combustion products can reinforce the effect of the ”flame” spike.

The results presented in Fig. 1.18c illustrate that combustion of H_2/boron composition has essential advantages, if compared with combustion of H_2/air mixtures: the ignition delays are by a order of magnitude shorter, and the temperature of combustion products is by 1000 K higher. It is in order to remark that the use of silane daes not affect the heat release in the reactions. In contrast to H_2/air mixtures, the increase in the initial pressure up to 5 bar does not affect much the auto-ignition process. All these factors are beneficial of the application of the H_2/boron compositions to increase the positive effect of the counterflow combustion on drag reduction of the blunt bodies in supersonic streams.

The theoretical and computational analysis has been carried out at the department of Thermo- and Fluid Dynamics of the Chalmers University of Technology.

1.5 Conclusions

- The theoretical and experimental study of counterflow combustion in supersonic streams confirms the fact that the ”flame” spike can be considered as an effective means to reduce the pressure drag of blunt bodies. Direct measurements of pressure drag have been carried out in the supersonic, M=2.0-2.5 air streams when the ”flame” spike has been formed with the help of counterflow combustion of hydrogen injected through the small pipe playing role of the structural spike. The spike with a conical tip having better flame stabilization capabilities has been also studied. The main mechanism of drag reduction has been analyzed with the help of numerical simulations.

  In experiments, the regions of stable counterflow combustion of hydrogen in the d (the blunt body diameter) - $\bar{L}$ (the dimensionless length of the spike) and $\bar{G}$ (the dimensionless hydrogen mass flow rate) - P_o (free stream stagnation pressure) planes have been determined. The main elements of the flow structure around the blunt body in the presence of inert and reactive injection have been resolved and measured.

- With the help of theoretical analysis, it has been established that the mechanism of drag reduction is mainly attributed to formation of the wake-type non-uniformity in the free stream initiated by injected hydrogen and reinforced by motion of combustion product behind the flame front propagating downstream in the deflagration regime of combustion.

  When pressure in the reaction zone increases (it can happen with an increase of the fuel mass flow rate or with an increase of free stream pressure), the hydrogen combustion becomes slower and less intensive that results in reduction of the positive effect of the ”flame” spike. To prevent this consequence, the moderation of pressure dependence of hydrogen combustion above the ”second extended limit of explosion” is proposed using silane or boron. In the case of boron, one can expect more rapid combustion as well as much stronger heat release effect. Both factors are beneficial of the drag reduction effect.

- The results of this study illustrating that the comparable efficiency in drag reduction can be achieved in the same wind tunnel under the similar flow conditions by using two different energy deposition methods - the optical (laser) discharge and counterflow hydrogen combustion. Thus, it may be argued that the phenomenon of drag reduction of blunt bodies in supersonic flows at atmospheric conditions is not plasma specific.

  The results illustrate the efficiency of counterflow combustion in drag reduction of blunt bodies in supersonic, M=2.0-2.5, flows. If realized, the technique could help in removing the controversial DU- projectiles from active applications.

Software developed or modified as a part of this project can be delivered if requested.

Acknowledgments

This work has been initiated by Dr. Ch. Raffoul in accordance with the contract SPC 00-4011.

Bibliography

[1] KANDEBO, S.W., "Air Spike" Could Ease Hypersonic Flight Problems, Aviation Week and Space Technology, May 15, 1995, p. 66

[2] TRETJAKOV, P.K., GOLOVITCHEV, V.I., AND BRUNO, C., Experimental and Numerical Study of Counterflow Jet Flame Stabilization in a Supersonic Air Stream, XII ISABE, Melbourne, September 10-15, 1995

[3] RIGGINS, D.W., NELSON, H.H., AND JOHNSON, E., Blunt Body Wave Drag Reduction Using Focused Energy Deposition, AIAA Paper 98-1647, 1998

[4] LEVIN, V.A., AFONINA, N.E., GEORGIEVSKIJ,P.YU., *et al.*, Impact of the Energy Source on Supersonic Flow around Blunt Bodies, Institute of Mechanics, University of Moscow, Preprint 36-98, 1998 (in Russian)

[5] BAEV, V.K., GOLOVITCHEV, V.I., TRETJAKOV, P.K., *et al.*, Combustion in Supersonic Flow, Nauka, Novosibirsk, 1984 (in Russian). Also NASA TM-77822, March 1985, also: GOLOVITCHEV, V.I., TRETJAKOV, P.K., Patent of Russian Federation RU 2029121, C1, 1995

[6] AMSDEN, A.A., KIVA-3: A KIVA Program with Block-Structured Mesh for Complex Geometries, LA-12503-MS, UC-231, March 1993

[7] GOLOVITCHEV, V.I., AND HANSSON, J., Some Trends in Improving Hypersonic Vehicles Aerodynamics and Propulsion, 14th International Symposium on Air-breathing Engines, September 5-10, 1999, Florence, Italy, Paper ISABE IS-90 (1999)

[8] BRUNO, C., GOLOVITCHEV, V.I., AND TRETJAKOV, P.K., New Trends in Improving Hypersonic Vehicles Aerodynamics and Propulsion: Flow Control by External Energy Supply, 21st ISTS, Omiya, Japan, Paper 98-o1-8V, 1998

[9] GOLOVITCHEV, V.I., AND BRUNO, C., Modeling of Parallel Injection Supersonic Combustion, Proceedings of the 19th International Symposium on Space Technology and Science, ed. by M. Hinada, AGNE Shafu Publ. Inc., Tokyo, p. 17, 1994

[10] GOLOVITCHEV, V.I., http://www.tfd.chalmers.se/˜ valeri/MECH.html, 1998

[11] NEVA PROJECT DESCRIPTION, http://www.sergib.agava.ru/russia/leninets/neva/neva.htm, 1999

[12] GOLOVITCHEV, V.I., AND BRUNO, C., Numerical Study of the Ignition of Silane/Hydrogen Mixtures, Journ. Propulsion and Power, vol. 15, No.1, pp. 92-96, 1999

[13] GUVERNUK, C.V., Personal communication, 1999

[14] GOLOVITCHEV, V.I., AND NORDIN, N., Detailed Chemistry Spray Combustion Model for the KIVA Code, The 11th International Multidimensional Engine Modeling User's Group Meeting, University of Wisconsin, March 4, 2001

”The Contractor, Chalmers University of Technology, hereby declares that, to the best of its knowledge and belief, the technical data delivered herewith under Contract No. F61775-00-WE011 is complete, accurate, and complies with all requirements of the contract.”

DATE:

_____

Name and Title of Authorized Official:

_____

”I certify that there were no subject inventions to declare as defined in FAR 52.227-13, during the performance of this contract.”

DATE:

_____

Name and Title of Authorized Official:

_____